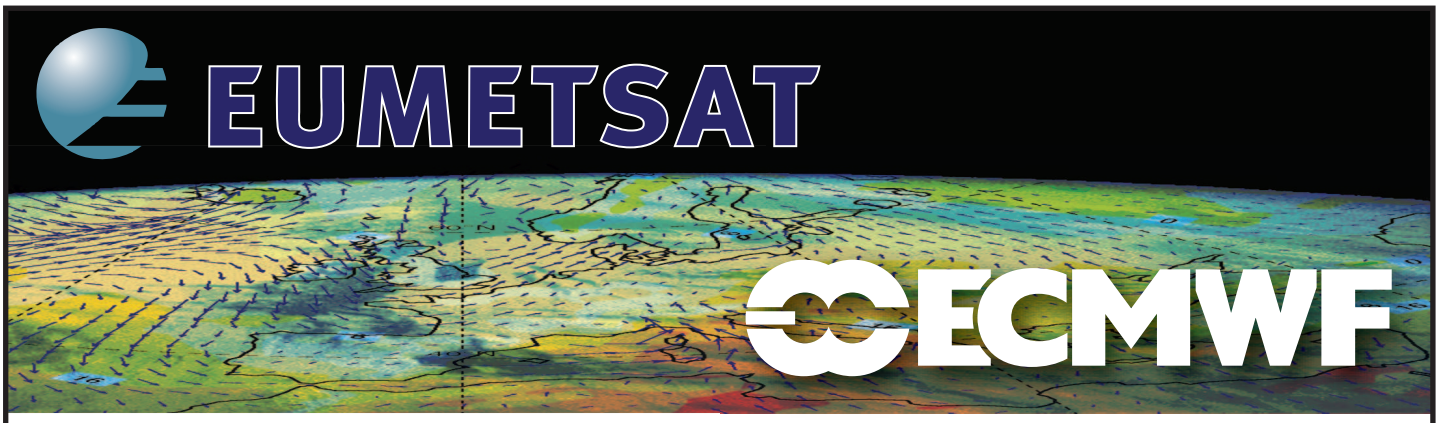

EUMETSAT/ECMWF Fellowship Programme
Research Report No. 31

Wind tracing with ozone-sensitive radiances from SEVIRI

Cristina Lupu and Anthony P. McNally

December 2013

Series: EUMETSAT/ECMWF Fellowship Programme Research Reports

A full list of ECMWF Publications can be found on our web site under:
http://www.ecmwf.int/publications/

Contact: library@ecmwf.int

European Centre for Medium Range Weather Forecasts
Shinfield Park, Reading, RG2 9AX, England

Abstract

Ozone-sensitive radiances from SEVIRI have been recently evaluated within the ECMWF operational system, both in terms of possibility of wind extraction from the 4D-Var assimilation and in terms of impact on analysis and forecast. To illustrate the effect of ozone feature tracing in the 4D-Var, experiments have been performed at ECMWF where the dynamical link between the ozone and the rest of the system has been deliberately enabled or disabled. The findings of this investigation show that, if the dynamical link between the ozone and the rest of the system is enabled, the 4D-Var has the freedom to change the temperature and wind fields, as well as the ozone field itself in order to improve the fit to observed ozone concentrations. SEVIRI ozone-sensitive observations, via passive tracing, provide a potentially useful constraint upon the analysis of wind, particularly in the upper troposphere and lower stratosphere. When added to an observation depleted baseline experiments, SEVIRI ozone-sensitive radiances changed the ozone analysis around 150 hPa and this improved the fit to MLS ozone data. The wind analyses scores are improved around 150 hPa, but the improvement is small when compared with the wind analysis scores from humidity-sensitive clear-sky radiances. When added to the full observing system, SEVIRI ozone-sensitive radiances slightly improves the fit to other infrared ozone-sensitive radiances, but the improvement is not visible in the fit to MLS. The wind analysis and forecast impact results do not suggest benefit on improving the ECMWF wind field.

1 Introduction

In recent years, a number of studies have investigated the value of assimilating ozone-sensitive infrared (IR) radiances from high spectral resolution infrared sounders (Han and McNally, 2010; Dragani and McNally, 2013). At ECMWF, Han and McNally (2010) showed that the assimilation of IASI ozone-sensitive radiances improve the agreement between the ozone analyses and independent data from MLS and sondes, particularly in the upper troposphere and lower stratosphere and at high latitudes in the Southern Hemisphere winter. Dragani and McNally, (2013) investigated the assimilation of the IR ozone-sensitive radiances from AIRS (flying onboard the NASA EOS Aqua satellite), IASI (EUMETSAT MetOp-A platform) and HIRS (flying onboard of the NOAA-17, NOAA-19 and EUMETSAT MetOp-A satellite) in combination with BUV data (from SBUV, OMI and SCIAMACHY). Results from this study have shown that the additional use of the IR ozone-sensitive channels does improve the ozone analyses compared to an assimilation based solely on BUV data. At ECMWF ozone-sensitive IR radiances from AIRS, IASI, and HIRS have been assimilated in the operational Integrated Forecasting System (IFS) since November, 2011.

Observations sensitive to temperature and moisture (IR/MW satellite radiances) can produce wind increments through the dynamic response to temperature and moisture increments in 4D-Var. Experience has already been gained in understanding the wind tracing capability of SEVIRI water vapour radiances in the 4D-Var. It has been demonstrated that in a 4D-Var data asimilation system, wind information can be derived from radiance observations, even though the radiances are not directly sensitive to tropospheric wind. Peubey and McNally (2009) showed that assimilation of humidity-sensitive clear-sky geostationary radiances from Meteosat-9 improve the 4D-Var wind analyses throughout the troposphere, with the strongest signal in the middle and upper troposphere. As described in Peubey and McNally, (2009) the most important mechanism through which the assimilation of clear-sky radiances constrains the analysis is the *humidity tracer advection* induced by 4D-Var, which dominate over the effects of balance constraints imposed on the analysis and model cycling. Lupu and McNally (2012) extended this study by demonstrating the effect of humidity-tracer advection involved in the production of wind increments from the cloud-affected Meteosat-9 SEVIRI observations.

An important benefit from the succesful extraction of ozone information from IR radiances is the possibility of constrainig the wind analysis field via the 4D-Var tracing. In particular, application of the 4D-Var methodology to time varying ozone-sensitive radiances measured by instruments on EUMETSAT geostationary satellites may provide unique information to constrain the wind analysis in the stratosphere. The SEVIRI imager, onboard Meteosat-9/-10 in geostationary orbit, has one channel (channel 8, centered in the 9.7 μm band) in the infrared spectral region that is sensitive to the ozone. Figure 1 shows the weighting functions for SEVIRI channels 4 to 11, for a satellite nadir view (Schmetz *et al.,2002*). SEVIRI ozone channel is sensitive to the atmospheric temperature profile, lower tropospheric water vapour, and the surface skin temperature and emissivity. Extracting wind information from SEVIRI ozone-sensitive radiances is an attractive and challenging prospect, particularly in the lower stratosphere, where few other observations of wind exist. The information lacks good vertical resolution. However, it is hoped that the very high temporal sampling of geostationary radiances will allow the motion of ozone features to be tracked to provide wind information.

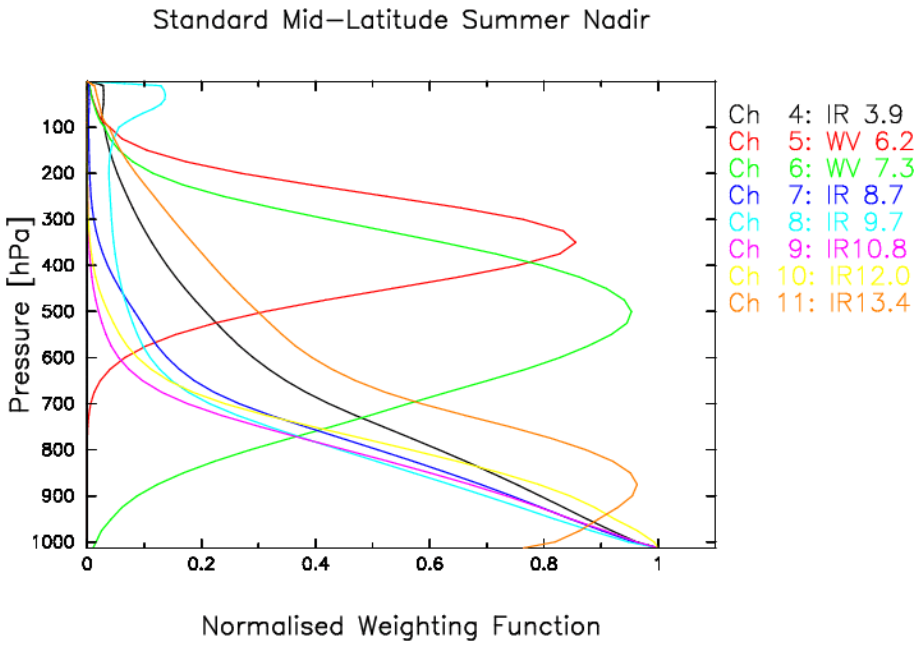

Figure 1: Weighting functions for SEVIRI channels 4 to 11, for a satellite nadir view for a standard midlatitude summer reference profile. Figure courtesy of EUMETSAT, Schmetz et al., 2002 .

This study intends to present preliminary answers to the following questions:

- Can ozone feature tracing information be extracted from SEVIRI ozone-sensitive radiances with a view to providing information to constrain the wind analysis in the stratosphere ?
- Can we succesfully exploit SEVIRI ozone-sensitive radiances to improve the ECMWF wind analysis field?

Although in theory ozone-sensitive radiances from satellites measurements may contain useful dynamical information (Daley, 1995; Peuch *et al*, 2000; Semane *et al.*, 2009), the overall aim of this study is to examine the wind tracing with SEVIRI ozone-sensitive radiances in an operational NWP context.

2 Illustrating wind tracing with SEVIRI ozone channel

In the current operational version of the ECMWF 4D-Var, ozone is analysed simultaneously with all the other analysis variables, but there is no dynamical coupling between ozone and other meteorological variables (Dethof and Hólm, 2004). That is to say ozone is analysed univariately: the background error covariances have no cross-correlations with ozone which means that there are no ozone increments from the analysis of the dynamical fields. In addition, the assimilation of ozone observations cannot modify the wind field in 4D-Var through the adjoint calculations. This step was taken to prevent large erroneus wind and temperature adjustements in the stratosphere associated with the assimilation of biased ultra violet observations under certain conditions (Dragani, 2011). The reader is refered to Dragani and McNally (2013) for details on the current ozone analysis system at ECMWF.

The aim of this section is to illustrate how 4D-Var accomodates observed local changes in ozone concentration by modifying the flow. To further illustrate the ozone-wind extraction in 4D-Var, two single cycle experiments on 1 June 2010 at 12 UTC have been run, starting from a depleted observing system baseline assimilating no observations other than conventional observations, scatterometer data and data from six GPS-RO sensors. Both experiments add SEVIRI ozone-sensitive radiances from channel 8 on top of that baseline, one with the ozone tracing enabled and one with the ozone tracing disabled. These experiments were performed with model cycle CY36R2 of the Integrated Forecasting System (IFS) at a reduced horizontal resolution T511 wavenumber truncation (40 km), and 91 vertical levels with a model top level pressure of 0.01 hPa.

Figure 2 shows the mean observed minus background radiance departure for SEVIRI clear-sky radiances (CSR) in channel 8 in a single assimilation cycle on 1 June 2010, from 9 UTC to 18 UTC. Two regions are marked in the picture: one with negative departures (blue dashed oval), where the background calculated radiances are warmer than the observations that indicate that the background is deficient in ozone concentration and one with positive departures (red dashed oval) that indicate the opposite.

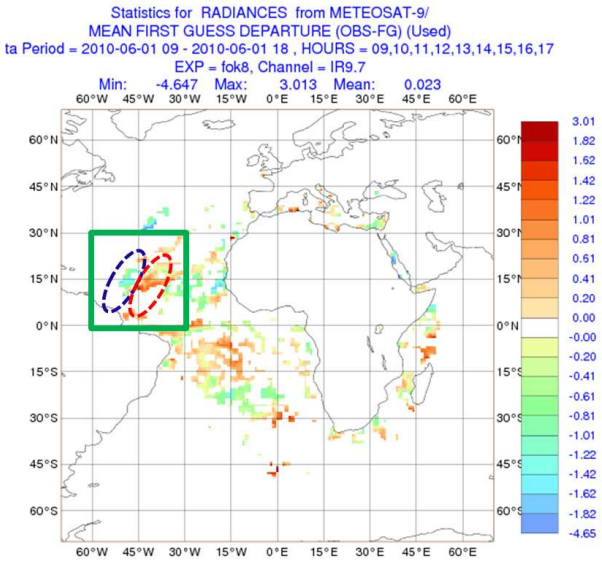

Figure 2: Mean observed-minus-background radiance departures (K) for SEVIRI CSR in channel 8 from 9 UTC to 18 UTC during the first assimilation cycle on 1 June 2010.

By assimilating SEVIRI data, the 4D-Var has, in principle, the freedom to change any aspect of the model initial state (e.g., temperature, wind fields, ozone field itself) in order to improve the fit to observed radiances later in the assimilation window. When the ozone feature tracing is disabled by explicitly zeroing any gradient of the ozone data fit with respect to changes in the initial wind field, the 4D-Var produce ozone increments only.

Figure 3 shows SEVIRI analyzed ozone mass mixing ratio and wind increments differences at 150 hPa generated by the assimilation of Meteosat-9 SEVIRI CSR from channel 8 with respect to the BASE in a single 4D-Var cycle, on 1 June 2010 at 18 UTC as obtained from the experiment where the ozone feature tracing was disabled or enabled, zoomed in on a region between about 0°and 30°N latitude and 30°W to 60°W longitude. It can be seen that by activating the ozone feature tracing, wind increments are generated by the 4D-Var to accomodate the differences between the ozone model background and the observations. There is clear evidence that the fitting of ozone-sensitive radiances within the 4D-Var analysis can be achieved by instigating ozone advecting wind increments, suggesting there is potential for these data to provide useful information on the wind field in the stratosphere.

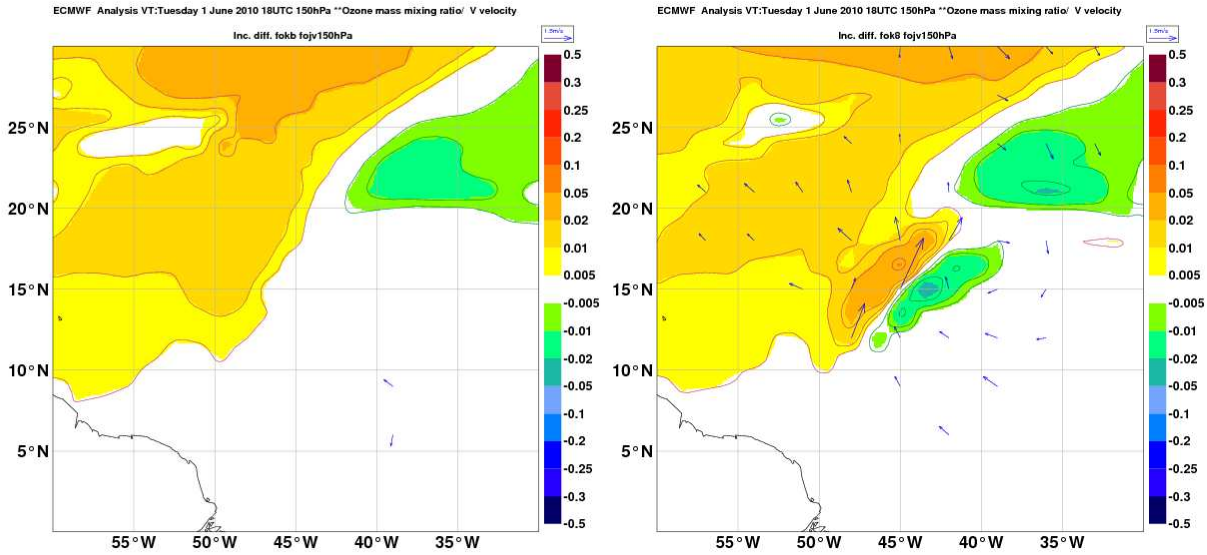

Figure 3: 150 hPa SEVIRI analyzed ozone mass mixing ratio differences ($mgkg^{-1}$) and wind increment differences (ms^{-1}) between the experiment assimilating SEVIRI CSR from channel 8 and the baseline on 1 June 2010 at 18 UTC: experiment with tracing disabled (left side) and experiment with tracing enabled (righ side).

3 Assessing the impact of SEVIRI ozone channel in a depleted observing system

Having demonstrated the potential for ozone tracing we now investigate the influence of SEVIRI ozone-sensitive radiances in ECMWF data assimilation system. A common methodology used to emphasise the impact of adding a single instrument or channel in the assimilation system is to conduct experiments in an observation depleted-system. In such a system, we can attribute any changes directly to the new added observations.

The following experiments with the ozone tracing effect enabled, have been run over the period 1 May

2010 - 1 July 2010:

- **BASE:** includes a depleted observing system in which no radiance and AMVs data from geostationary or polar-orbiting instruments has been assimilated. Assimilated observations are therefore only conventional observations, scatterometer data and GPS radio occultation data.
- **MET9WV:** As BASE, but with SEVIRI CSR from Meteosat-9 water-vapour channels 5 and 6 added.
- **MET903:** As BASE, but with SEVIRI O3 sensitive radiances from Meteosat-9 channel 8 added.
- **MET9WV+O3:** As BASE, but with SEVIRI CSR from Meteosat-9 channels 5, 6 and 8 added.
- **BUV:** As BASE, but with BUV data added (total column ozone from the Aura OMI and ENVISAT SCIAMACHI instruments, partial columns retrieved from NOAA-17 and NOAA-18 SBUV/2).
- **BUV+MET9O3:** As BASE, but with BUV and SEVIRI channel 8 ozone-sensitive radiances added.

3.1 Fit to ozone estimates from Aura MLS

Figure 4 shows the impact of MET903, BUV and BUV+MET9O3 on ozone in terms of zonally averaged mean analysis differences with respect to BASE. When SEVIRI radiances from channel 8 are assimilated, changes in the ozone analyses are found in the Tropics, mainly in a region between 10 hPa and 100 hPa and in the Southern Hemisphere midlatitudes in a layer between 100 hPa and 200 hPa (Figure 4, top panel). The use of BUV data (and similar BUV+MET9O3) produces changes in the Tropics above 50 hPa and in the higher latitudes in both hemispheres around 100 hPa to 200 hPa.

To assess if the changes introduced by each observing system correspond to an improvement or degradation of the ozone analyses, we look at how these changes influence the fit of the resulting ozone analyses to ozone estimates from the MLS. Figure 5 shows the comparison of the ozone analyses with the reprocessed MLS ozone profiles in terms of their zonal mean differences and their standard deviations. The main findings are:

- In the Tropics, the BASE system displays a strong underestimation of ozone in a deep layer between 10 hPa and 100 hPa. The Meteosat-9 ozone-sensitive radiances are sensitive to the understimation and correct accordingly. The use of BUV data also add ozone around 30 hPa improving the fit to MLS.
- In the Southern Hemisphere midlatitudes the BASE system display an overestimation of ozone at 10 hPa and an underestimation a few levels below at 30 hPa. The use of MET9O3 slightly improve the fit to MLS below 50 hPa but fail to improve the fit to MLS above 50 hPa. The BUV data add ozone around 30 hPa that degrade the MLS fit.
- In the Northern Hemisphere midlatitudes, the comparison of BASE with MLS indicates an overestimation of ozone centered around 20 hPa and an underestimation above and below. The BUV data add ozone around 30 hPa that degrade the MLS fit. The use of both BUV+MET9O3 data do a very similar job compared to BUV data alone over all regions.

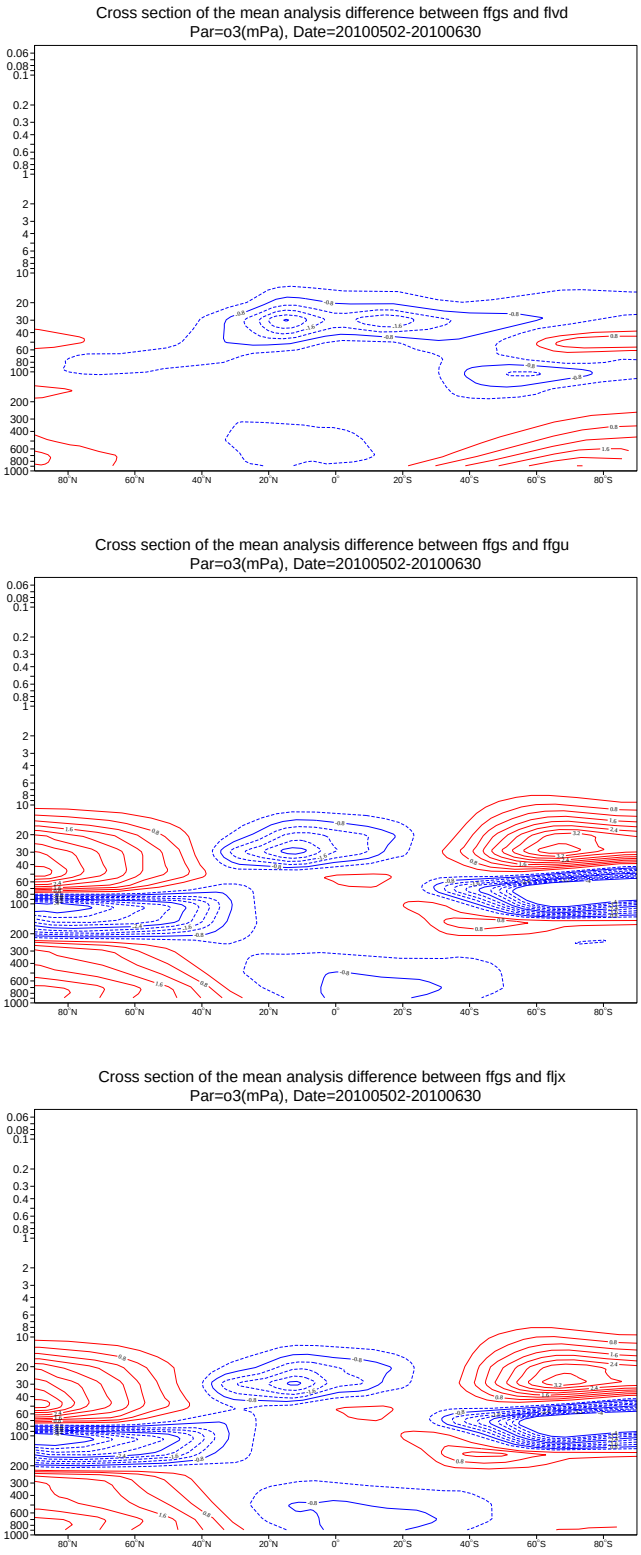

Figure 4: Latitude-pressure cross-section of ozone analysis differences computed between BASE and each of the experiments MET903, BUV and BUV+MET9O3. The differences are computed over May-June 2010 period. Dashed lines denote negative values (i.e. the experiment have larger values than the BASE). Ozone data are in mPa. Contours are plotted with intervals of 0.4 mPa.

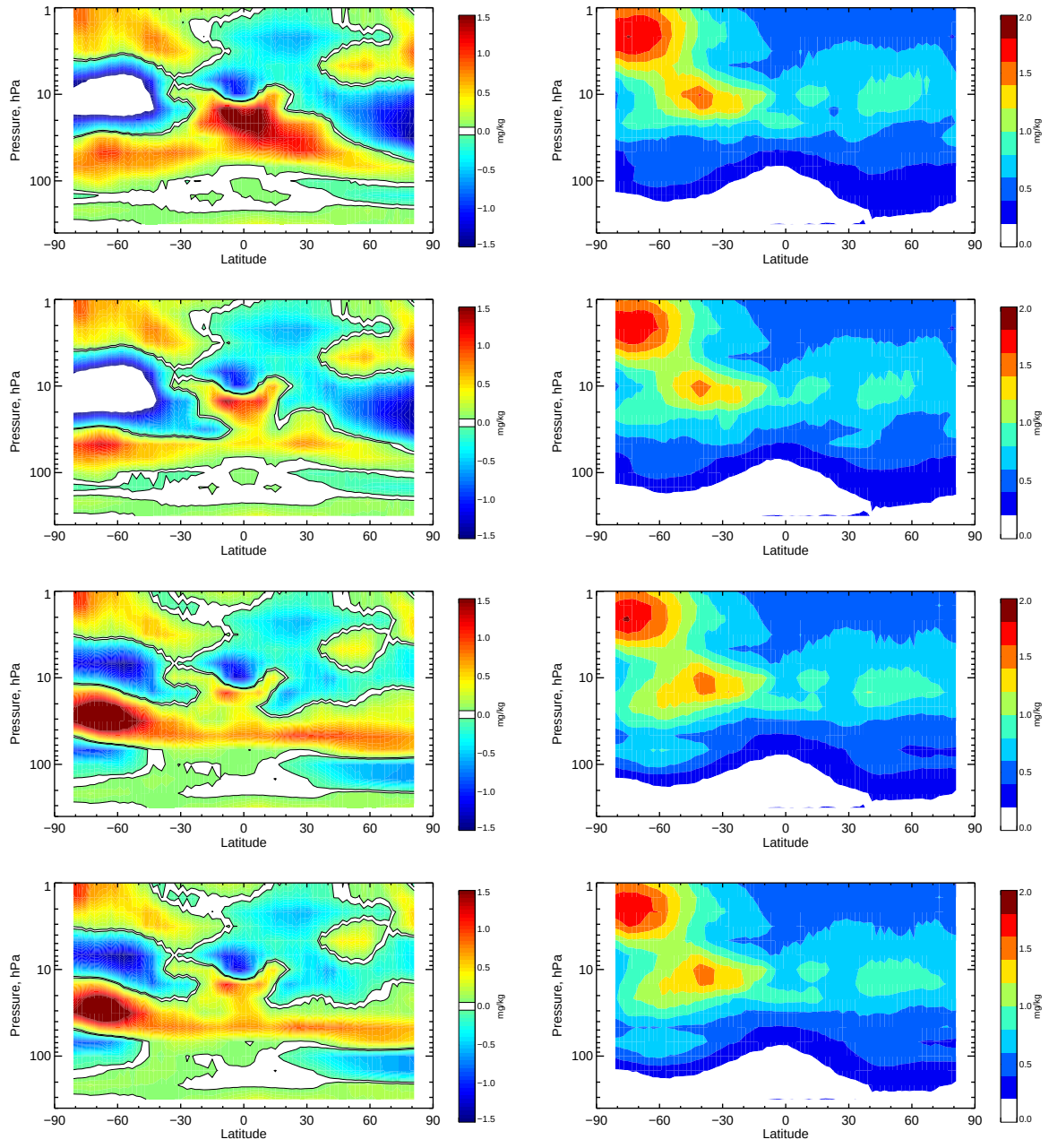

Figure 5: Mean (left panels) and standard deviation (right panels) difference between the MLS ozone profiles and the co-located ozone analyses computed for BASE (top), MET903 (second row), BUV (third row) and BUV+MET9O3 (bottom) averaged over the periods 1 May -1 July 2010. Data are in mass mixing ratio (ppmm).

3.2 Wind analysis increments

We display the analysis impact of different ozone observations in terms of the root-mean-square (RMS) wind increments difference with respect to the BASE assimilation (Fig. 6). Changes to the RMS wind increments are shown as vertical profiles on pressure levels between 100 hPa and 10 hPa averaged inside Meteosat-9 disc area. For reference MET9WV is also shown. As expected from previous studies, WV CSR have the maximum impact on the wind analysis in the troposphere at 500 hPa. MET9O3 data have a small impact on the wind analyses when compared with humidity-sensitive CSR, showing a main peak in the upper troposphere. When MET9O3 are assimilated in addition to WV CSR or BUV ozone data, the additional impact on wind analyses in the upper troposphere is very small.

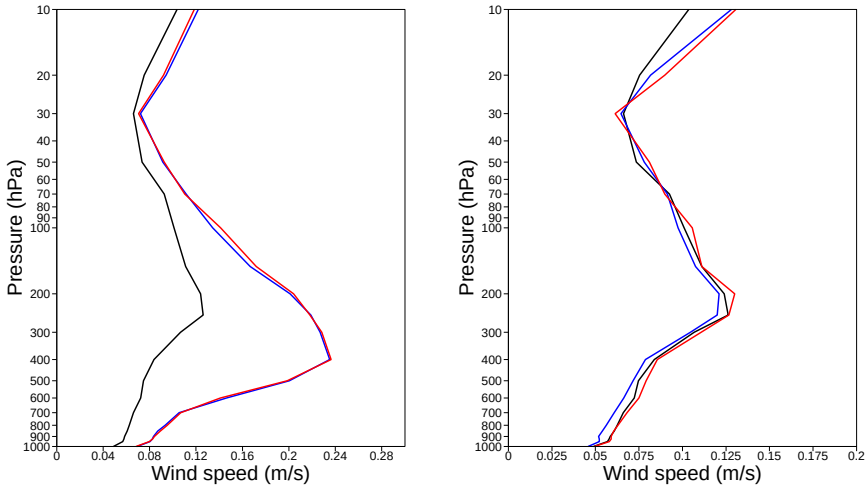

Figure 6: RMS of wind speed increment differences between each of the experiments and the BASE: a) MET903 (black line), MET9WV (blue line), MET9WV+O3 (red line); b) MET903 (black line), BUV (blue line) and BUV+MET9O3 (red line).

Figure 7 shows the vector difference of the mean wind analysis at 150 hPa between MET9O3 experiment and the BASE. Small wind changes are seeen in the Tropics where the differences in the mean field are less than 1 m/s. In the midlatitudes the magnitude of the changes is typically less than 0.5 m/s.

3.3 Wind analyses scores

Wind analyses scores measure ability to reproduce operational wind analysis (considered as the best available estimate of the true wind field) using reduced observations.

In the following, wind analysis scores are calculated for each experiment inside Meteosat-9 disc by averaging over all m assimilation cycles (Peubey and McNally, 2009) :

$$\Delta\overline{RMSE} = \frac{\sum_{j=1}^{m}(RMSE_j^b - RMSE_j)}{\sum_{i=j}^{m} RMSE_j^b}. \quad (1)$$

where $RMSE_j$ and $RMSE_j^b$ are the wind analysis error for experiment and for the baseline, respectively. For every cycle j, wind analysis errors are calculated as departures from the ECMWF operational anal-

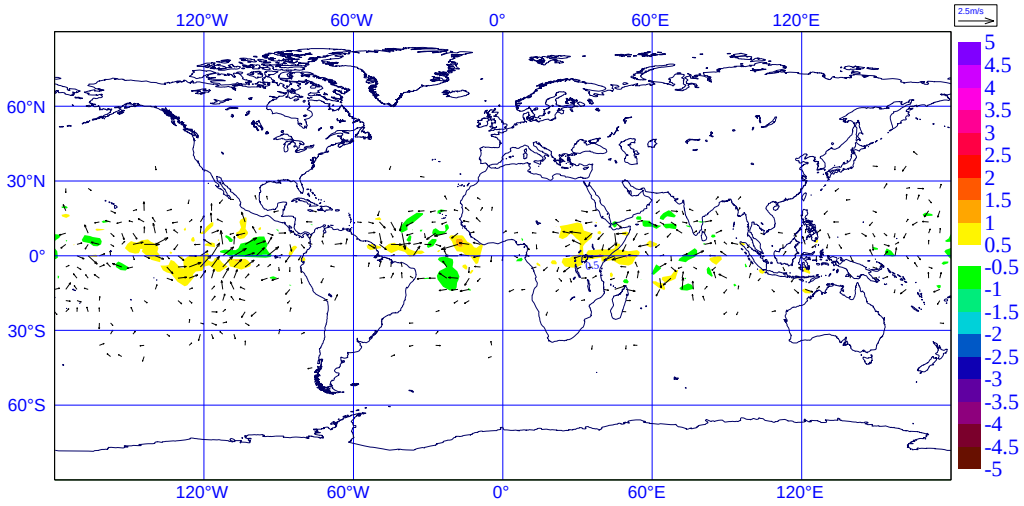

Figure 7: Difference in the mean wind analysis at 150 hPa between MET9O3 experiment and BASE. Shadding indicate the difference in mean wind speed [m/s]. The considered period is 1 May 2010 -1 July 2010.

ysis that runs at T1279 resolution and assimilate the entire observing system as:

$$RMSE_j = \sqrt{\frac{1}{n}\sum_{i=1}^{n}(u_i - u_i^r)^2 + (v_i - v_i^r)^2}, \tag{2}$$

$$RMSE_j^b = \sqrt{\frac{1}{n}\sum_{i=1}^{n}(u_i^b - u_i^r)^2 + (v_i^b - v_i^r)^2}, \tag{3}$$

where u_i and v_i (u_i^b and v_i^b) are the analysis values of the zonal and meridional wind components at a grid point i for the experiment (baseline), u_i^r and v_i^r are the corresponding values from the ECMWF operations and n is the number of grid points inside the considered area (longitude within 50°W-50°E, latitude within 20°N-50°N for the Northern Hemisphere, 20°S-20°N for the Tropics and 50°S-20°S for the Southern Hemisphere).

When a data set is added to the baseline the resulting analysis is always expected to perform better when compared to this baseline. A zero value of the analysis score means no improvement over the low resolution (T511) baseline while a 100% value corresponds to an analysis that has no error with respect to the high resolution (T1279) operational analysis. The wind analysis scores are here limited by the use of the T511 resolution and can never reach 100%. The best possible scores obtained by running the operational suite at T511 are around 60% in the Northern Hemisphere and Tropics and 80% in the Southern Hemisphere (Peubey and McNally, 2009).

Figure 8 shows the wind speed scores for all experiments described in the previous section. Vertical error bars superimposed upon the plot indicate 95% confidence interval for wind analysis scores and were calculated using the t-test distribution as in Peubey and McNally (2009).

Consistent with previous studies (Peubey and McNally, 2009; Lupu and McNally, 2012), the best scores for WV CSR are found at 300 hPa and 500 hPa, which correspond to the maxima of the two WV channel weighting functions (not shown). At levels above 250 hPa where CSR have little direct sensitivity, the MET9WV scores are still positive. The MET9O3 data only measurably improve the wind analysis at 150 hPa in the Tropics, but even here the impact is small (2%) when compared with the impact of WV

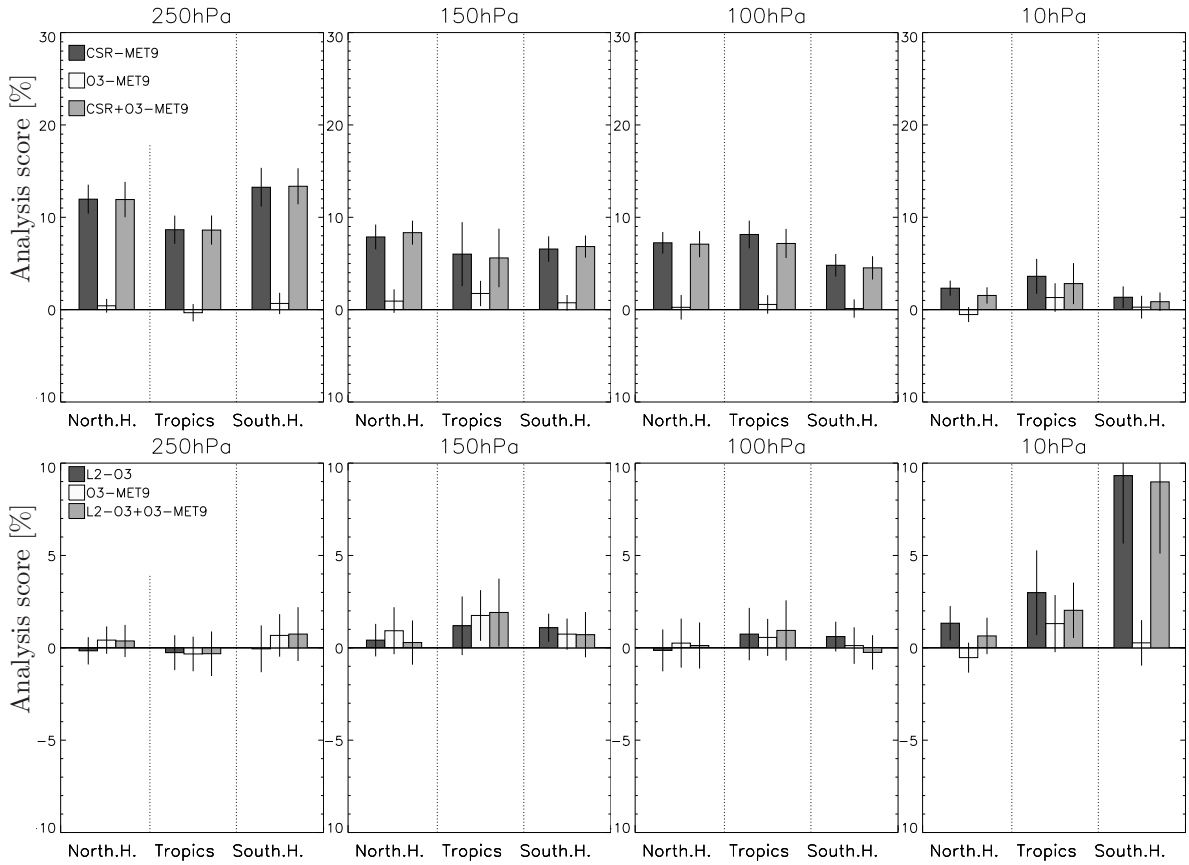

Figure 8: Wind analysis scores calculated inside Meteosat-9 disc in the Northern Hemisphere [20°N-50°N], Tropics [20°S-20°N] and in the Southern Hemisphere [50°S-20°S]. Top: MET9WV (black), MET9O3 (white), MET9WV+O3 (dark grey); Bottom: BUV ozone products (total column ozone from the Aura OMI and ENVISAT SCIAMACHI instruments and partial columns retrieved from NOAA-17 and NOAA-18 SBUV/2) (black), MET9O3 (white) and both BUV+MET9O3 (dark grey). In all experiments the ozone feature tracing was enabled. Each pannel refer to a given tropospheric pression level.

CSR. Ozone BUV data appear to have their maximum impact on wind analysis up to 10% much higher in the middle stratosphere (around 10 hPa).

3.4 Forecast impact

To investigate if METO3 have any impact on the NWP forecast, scores are calculated as normalised difference in root mean square errors between the each forecast experiment (e.g., MET9O3) and the coresponding reference forecast experiment (e.g., BASE). Experiments are verified against operational analysis. Figure 9 show the effect on RMS forecast scores for vector wind over an 60 day experimental period. SEVIRI channel 8 assimilation makes small but significant degradation at T+12 to T+48 in the Tropics in the lower troposphere at 700 hPa, counterbalanced by small significant improvement at T+12 in the Tropics at 500 hPa. In the extra-tropics, the forecast impact from the assimilation of MET9O3 data is overall neutral.

The comparison with an observation depleted observing system (e.g., BASE) does not give a realistic representation of the forecast improvements to be expected when ozone-sensitive SEVIRI radiances are

added to a full observing system. To further characterise the forecast impact of SEVIRI channel 8 radiances, the next section discusses results from additional assimilation experiments conducted in a full observing system where the analysis error are small.

4 Assessing the impact of the SEVIRI ozone channels in a full observing system

Previous experiments showed the impact of METO3 data in a depleted observing system. We now evaluate the value of assimilating ozone-sensitive infrared radiances from Meteosat-9 in a full operational observing system environment.

In the following, experiments were carried out with a recent version of ECMWF model cycle 38R2, implemented operationally on 25 June 2013 (Bauer *et al*, 2013). Experiments were conducted over a period covering 1 June - 31 August 2012 and use ECMWF 12-h 4D-Var system, with a spatial model resolution of T511 (horizontal resolution roughly 40 km) and 137 vertical levels with the model top at 0.01 hPa. Ten-day forecasts were calculated from each 00 Z analysis. The experiments use the full operational observing system assimilated operationally at ECMWF at the time. This includes conventional observations, polar orbiting satellite measurements (IASI, AIRS, ATMS, AMSU-A, AMSU-B, MHS, SSMIS, TMI, ASCAT), geostationary radiances and wind vectors and bending angles from the COSMIC constellation, METOP-A and TERRA-SAR-X. Note that in this configuration SEVIRI all-sky radiances are assimilated that now includes clear and overcast observations in two water vapour channels (Lupu and McNally, 2012). Ozone data from a number of instruments are also assimilated in the ECMWF system. This include level 2 ozone data from three SBUV/2 instruments (on board NOAA-17, NOAA-18 and NOAA-19) in the form of partial column over six vertical layers, and total column ozone retrieved from SCIAMACHY and OMI. Ozone-sensitive IR channels from 16 IASI channels, 19 AIRS channels and one HIRS channel are also operational assimilated since November 2012. Two of these channels (i.e., AIRS channel 1088 and IASI channel 1585) are used to anchor the ozone bias correction, together with SBUV/2 partial ozone columns (Dragani and McNally, 2013).

The following experiments have been performed:

- **CTRL:** use the full observing system assimilated operationally at ECMWF at the time.
- **CTRL_ON:** As CTRL experiment except that ozone feature tracing was enabled.
- **MET9ch5:** As CTRL, but additionally include SEVIRI ozone-sensitive radiances from channel 8 over ocean surfaces excluding CSR observations having a percentage of cloudy pixels more than 30 %, as well as CSR over high terrain and with satellite zenith angles larger than 60 °. SEVIRI ozone channel is bias corrected with a flat global offset (Dee, 2004). A value of 2 K has been assigned to the observation error standard deviation in this channel.
- **MET9ch5_ON:** As MET9ch5 experiment except that ozone feature tracing was enabled.

4.1 Changes to the ozone analysis

We now compare the various ozone analyses to independent, unassimilated ozone observations from MLS. Figure 10 shows the comparison to MLS ozone profiles in terms of their zonal mean differences and their standard deviations. It can be seen from CTRL and CTRL_ON experiments that, enabling the

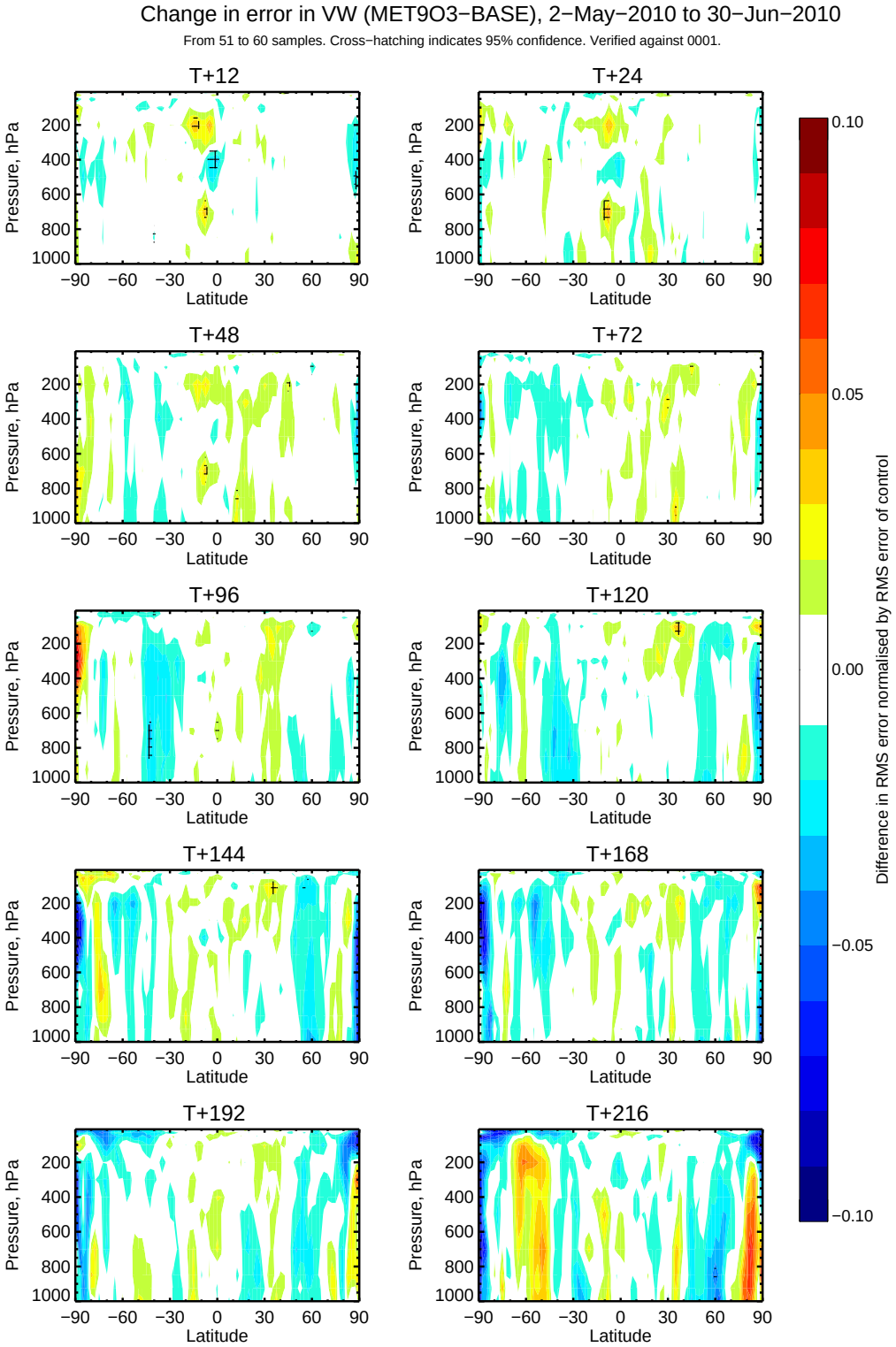

Figure 9: Normalised change in the RMS of vector wind forecast error between the MET9O3 experiment and the BASE. Verification is against the operational analysis and scores are based on a two month period, May to June 2010. Cross-hatched areas show changes that are significant at the 95% confidence interval. A beneficial impact is one that results in a reduction in forecast error,i.e.a negative normalised change. This is indicated by blue colours.

ozone tracing, doesn't impact the quality of the ozone analyses with existing ozone observations. In addition, results from CTRL_ON and MET9ch5_ON experiments show that in the full system experiments with many existing ozone observations, the assimilation of SEVIRI channel 8 does not have any additional impact on ozone analysis.

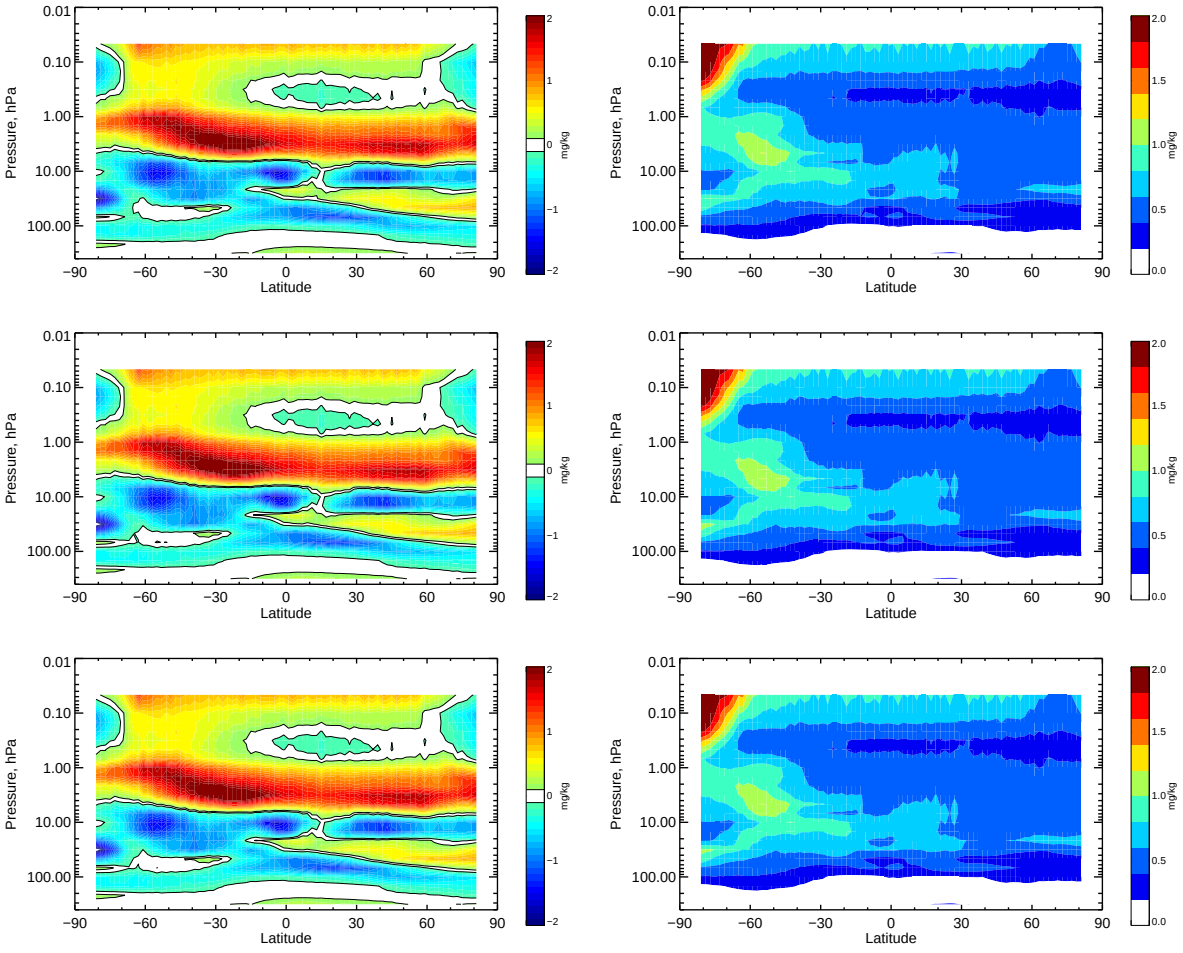

Figure 10: Mean (left panels) and standard deviation (right panels) difference between the MLS ozone profiles and the co-located ozone analyses computed for CTRL (top), CTRL_ON (second row), MET9ch5_ON (bottom) averaged over the periods 1 June - 31 August 2012. Data are in mass mixing ratio (ppmm).

Fits to the ozone-sensitive channel 9 of HIRS and ozone-sensitive channels of IASI also have been examinated. Figure 11 shows the normalised standard deviation of departures for global HIRS observations from NOAA-19 and Metop-A. The MET9ch5_ON and MET9ch5 experiments reduce the standard deviation of first-guess (FG) departure in HIRS ozone channel by around 0.8 % indicating improved ozone fields. The improvements are present in both tropics and extra-tropics, and are largest in the tropics (not shown). In the analysis, fits to HIRS ozone channel are improved by around 2.2% and 1.7%, respectively and are statistically significant. The CTRL_ON experiment sligtly increases the standard deviation of FG departure by up to 0.2%, while in the analysis, it is interesting that fit to HIRS ozone channel are improved by up to 0.2%.

Similar results are seen in the fits to ozone-sensitive channels of IASI, though these improvements are smaller and are not statistically significant (not shown).

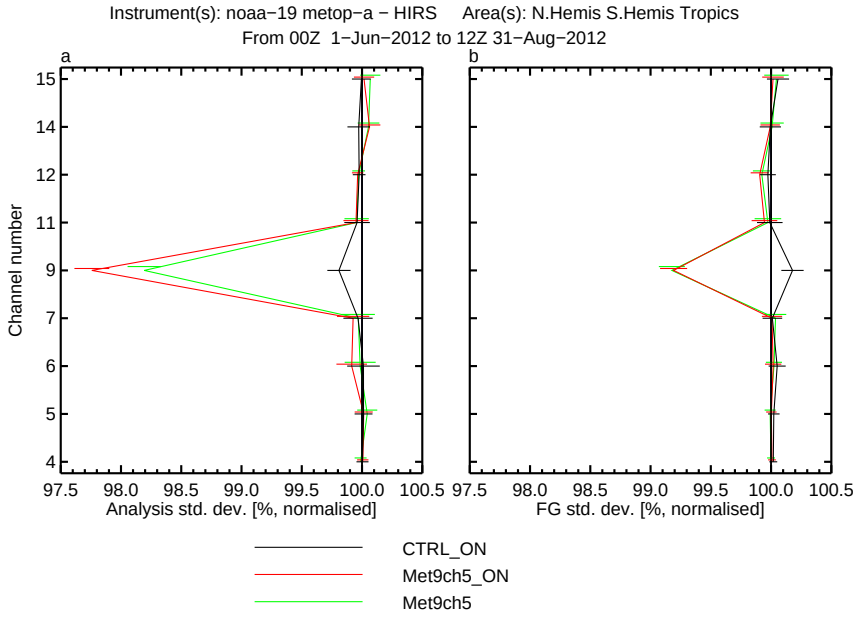

Figure 11: Normalised change in standard deviation of analysis (left) and first-guess (right) forecast departures for global HIRS observations from NOAA-19 and Metop-A. Standard deviations are normalised by those of the control experiment. Error bars indicate the 95% confidence interval. Numbers less than 100% indicate beneficial impact.

4.2 Changes to the wind analysis

The experiment CTRL_ON tests the impact of enabling the ozone tracing with the existing observation network, while MET9ch5_ON and MET9ch5 respectivelly, test the impact of the additional SEVIRI channel 8 radiances with the tracing enabled or disabled. We will now compare each of the experiments with the CTRL to characterise the changes in wind analysis.

Comparison of the mean wind analysis between each of the previous experiments and CTRL reveals some changes in the upper troposphere on levels between 100 hPa and 200 hPa, where the magnitude of the differences is mainly less than 0.5 m/s (not shown). At all other levels, there are no measurable changes in the mean wind field.

Figure 12 shows the normalized standard deviation of departures for conventional observations of wind over the globe. CTRL_ON and MET9ch5_ON reduce the standard deviation of FG in the upper-troposphere between 100 hPa and 150 hPa, while MET9ch5 increase the standard deviation of FG at 200 hPa by around 0.4%. In the analysis changes are not statistically significant.

Figs. 13 and 14 show the normalized changes in RMS errors in vector wind as a function of latitude and pressure as obtained from the experiments CTRL_ON and MET9ch5_ON. Results suggest that both experiments slightly decrease the RMS error at shorter ranges, but the changes are not statistically significant meaning that enabling the ozone tracing in 4D-Var will not results in improvements to the quality of wind forecasts at shorter ranges. Though for CTRL_ON experiment in longer ranges, the overall impression is that the RMS wind error increase.

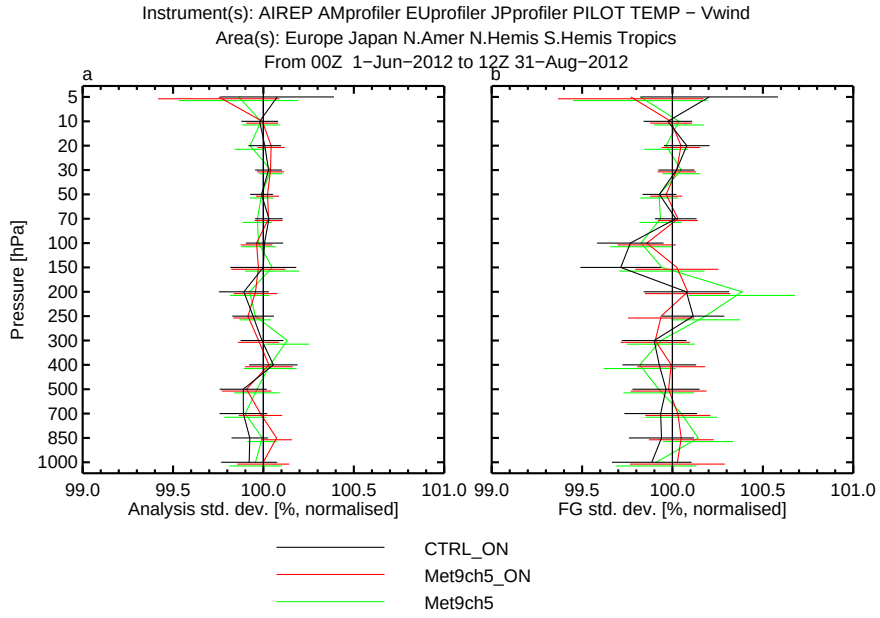

Figure 12: Normalised change in standard deviation of analysis (left) and first-guess (right) forecast departures for radiosonde, aircraft and pilot v-wind observations. Standard deviations are normalised by those of the control experiment. Error bars indicate the 95% confidence interval. Numbers less than 100% indicate beneficial impact.

4.3 Forecast verification

Figure 15 show the normalised difference in geopotential RMS error for the CTRL_ON, MET9ch5_ON and MET9ch5 experiments. The experiment CTRL_ON isolates the impact of ozone feature tracing, suggesting that coupling ozone with dynamics degrades the forecast scores, particularly in the Northern Hemisphere after the day 3 range. Comparing MET9ch5_ON and MET9ch5 with CTRL isolates the impact of SEVIRI channel 8 with and without ozone tracing effect enabled. The impact on the 500 hPa geopotential is neutral to positive for the Southern Hemisphere and Northern Hemisphere in a short range, and neutral to negative in the Northern Hemisphere, particularly after the day 6 range. Overall, it appears that there are no further benefits in terms of forecast skills from the additional assimilation of ozone-sensitive SEVIRI observations.

5 Conclusions

This study reports on the first experiments at ECMWF with SEVIRI ozone-sensitive radiances, both in terms of possibility of wind extraction from the 4D-Var assimilation and in terms of impact on analysis and forecast.

In the first part of the study, we have illustrated the effect of ozone feature tracing in the 4D-Var. We have highlighted that, if the dynamical link between the ozone and the rest of the system is enabled, the 4D-Var has the freedom to change the temperature and wind fields, as well as the ozone field itself in order to improve the fit to observed ozone concentrations. Thus, ozone observations, via passive tracing, provide a potentially useful constraint upon the analysis of wind, particularly in the upper troposphere and lower stratosphere.

The impact of SEVIRI radiances from channel 8 has been evaluated both in terms of the impact on a

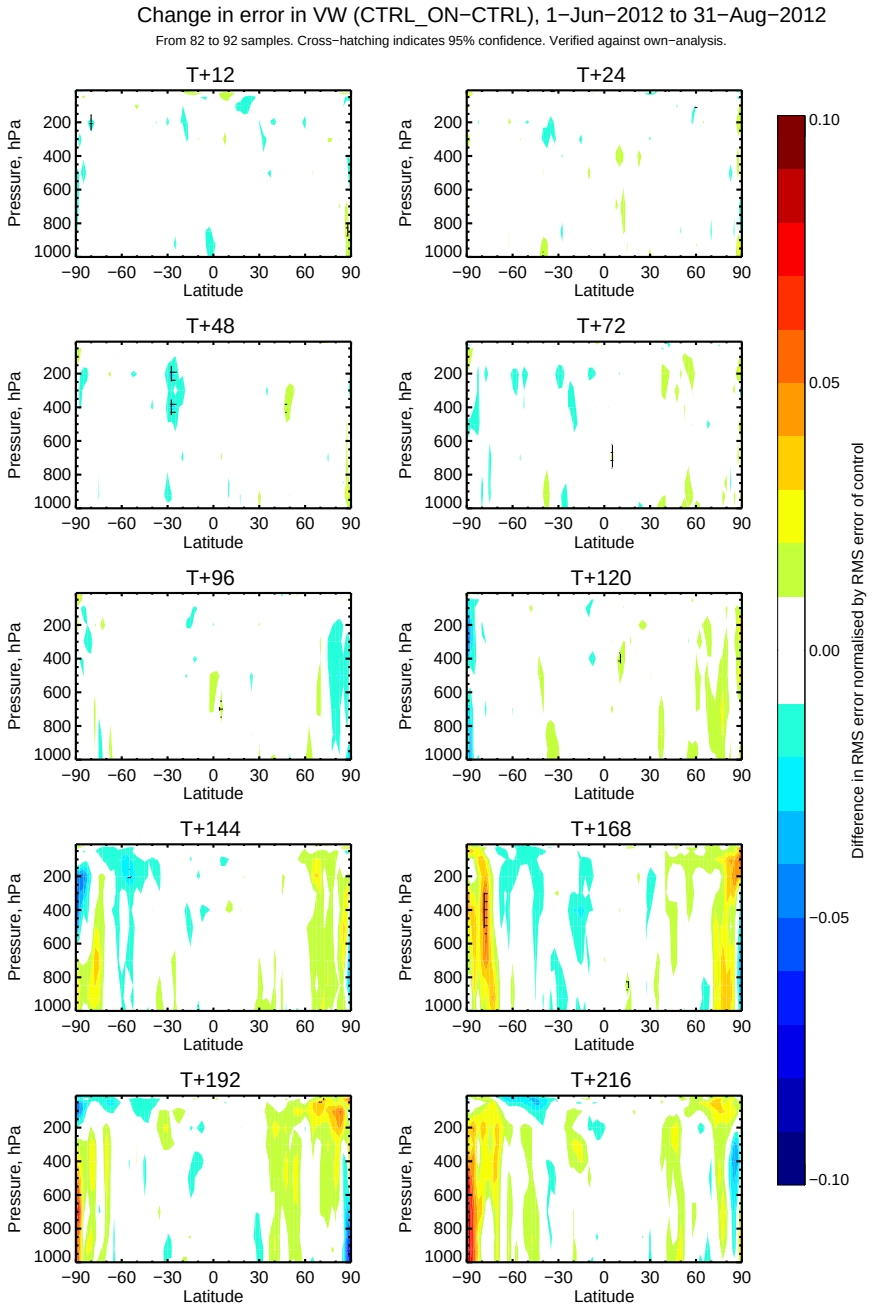

Figure 13: Zonal mean of normalized differences in the root mean square forecast error for the vector wind between CTRL_ON experiment and the CTRL control. Blue areas indicate reduced RMS forecast errors and hence improved forecasts; green/yellow/red areas indicate the opposite. Cross hatching indicates a statistically significant change.

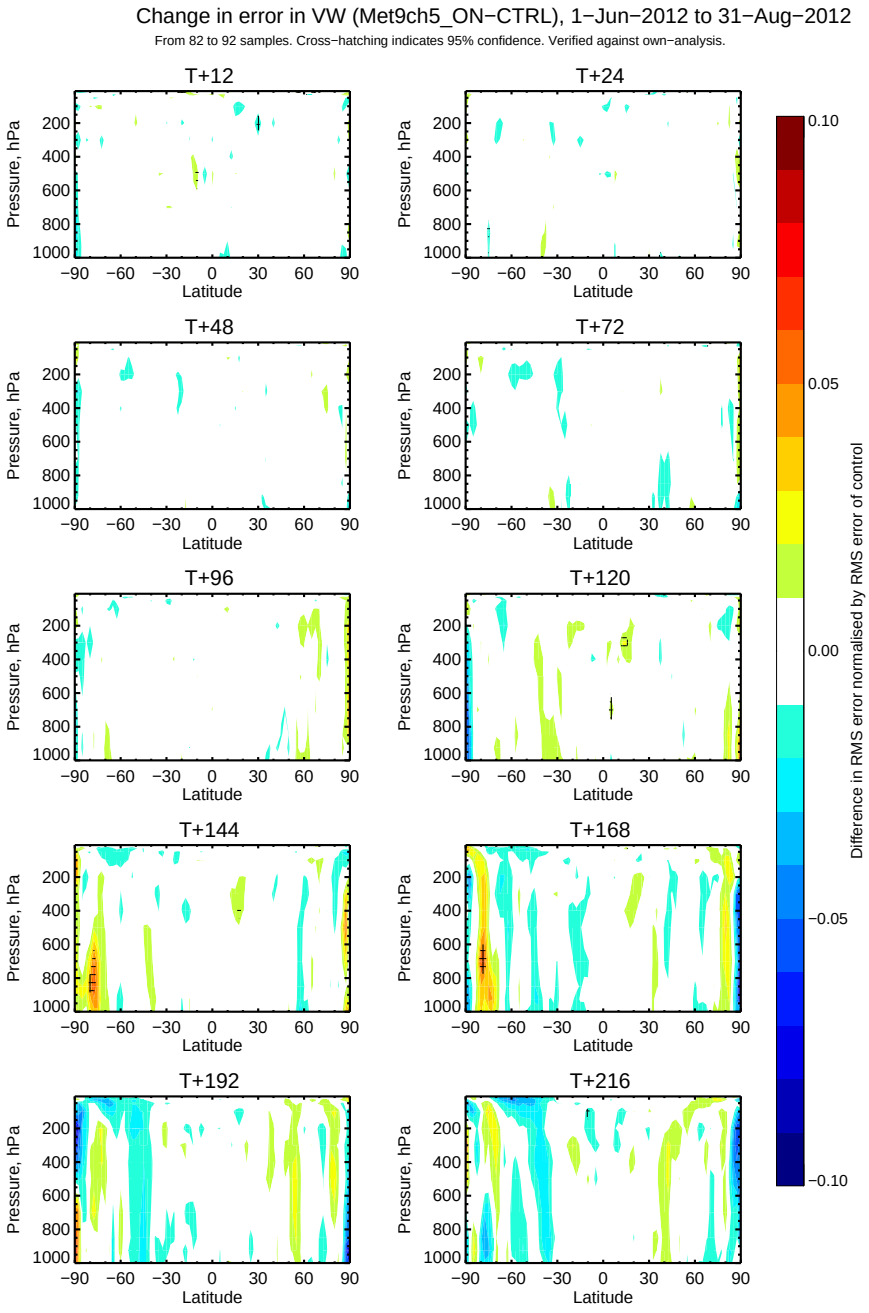

Figure 14: As Fig. 13 but for Met9ch5_ON and the CTRL experiments.

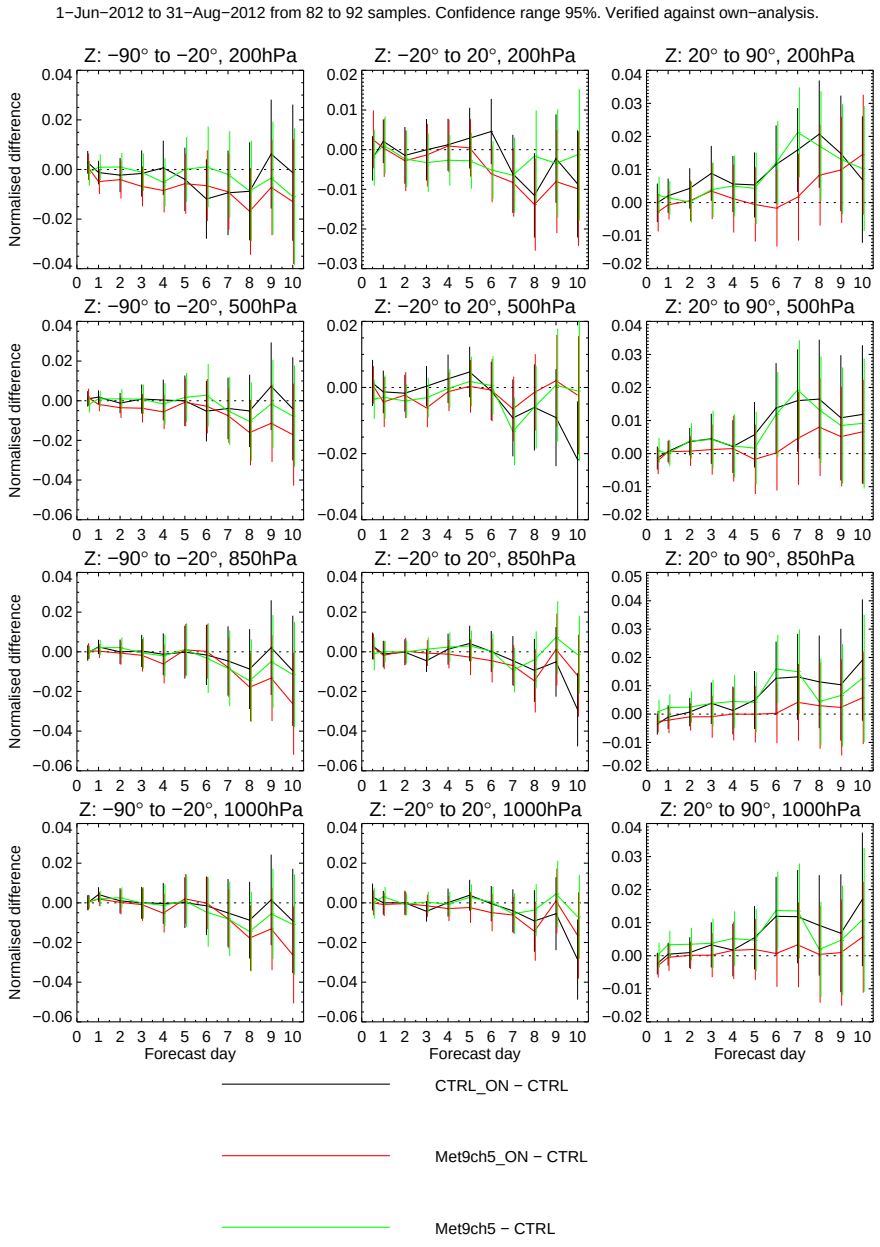

Figure 15: Normalised change in RMS forecast error in geopotential height at 200 hPa, 500 hPa, 850 hPa and 1000 hPa for the Southern Hemisphere, Tropics and Northern Hemisphere. Verification is against own analysis. Scores are based on a 3 month period, June to August 2012. Error bars indicate the 95% confidence interval.

depleted observing system as well as the impact in a full observing system. The results in a depleted observing system are encouranging and demonstrate that:

- In the absence of radiances data and AMVs from geostationary and polar orbiting satellites and of other ozone data, SEVIRI ozone-sensitive radiances changed the ozone analysis around 150 hPa and this improved the fit to MLS ozone data.
- SEVIRI channel 8 data improved the wind analyses scores around 150 hPa, but the improvement is small when compared with the wind analysis scores from humidity-sensitive CSR.
- The changes in the ozone and wind analysis are much smaller than equivalent for BUV data.

For the experiments in the full observing system, the addition of SEVIRI channel 8 ozone-sensitive radiances has to be viewed in the context of the many other ozone observations from a number of instruments already assimilated in the ECMWF system. The results highlight that:

- SEVIRI channel 8 slightly improves the fit to other IR ozone data (improved ozone) but the improvement is not visible in the fit to MLS.
- The wind analysis and forecast impact is neutral. There is no visible or significantly positive impact on improving the ECMWF wind field.

Since the results of the assimilation of SEVIRI ozone-sensitive radiances does not show significant improvements in the forecast scores, we do not suggest an operational change at ECMWF. As NWP systems improve it is becoming harder to demonstrate the beneficial impact of a single instrument or channel.

The use of SEVIRI data at ECMWF has been recently extended to assimilate overcast radiances in addition to CSR from WV channels (Lupu and McNally, 2012). Continuous effors are made at ECMWF to fully understand the behaviour of infrared instruments in the assimilation and to try to optimise their impact on forecast accuracy.

6 Acknowledgements

Cristina Lupu was funded through the EUMETSAT Fellowship Programme. We gratefully acknowledge Dr Rossana Dragani for providing helpful advice during the study and support with the MLS comparisons. Additional thanks go to Dr Elias Hólm and Dr Alan Geer for stimulating discussions and Dr Stephen English and Dr Jean-Nöel Thépaut for their constructive suggestions and review of the manuscript.

References

Bauer, P., A. Beljaars, M. Ahlgrimm, P. Bechtold, J.-R. Bidlot, M. Bonavita, A. Bozzo, R. Forbes, E. Hólm, M. Leutbecher, P. Lopez, L. Magnusson, F. Prates, M. Rodwell, I. Sandu, A. Untch, F. Vitart, 2013: Model Cycle 38r2: Components and Performance. Technical Memorandum 704, ECMWF, [available from http://www.ecmwf.int/publications/library/do/references/show?id=90759].

Daley, R., 1995: Recovery of the one and two dimensional windfields from chemical constituent observations using the constituent transport equation and an extended Kalman filter, *Meteorol. Atmos. Phys.*, **60**, 119-136.

Dee, D., 2004: Variational bias correction of radiance data in the ECMWF system, in ECMWF Workshop on Assimilation of High Spectral Resolution Sounders in NWP, 97-112, ECMWF, Reading, UK.

Dethof A. and E.V. Hólm, 2004: Ozone assimilation in the ERA-40 reanalysis project. *Q. J. R. Meteorol. Soc.*, **130**, 2851-2872.

Dragani, R., 2011: On the quality of the ERA-Interim ozone reanalyses: comparisons with satellite data. *Q. J. R. Meteorol. Soc.*, **137**, 1312-1326. doi: 10.1002/qj.821

Dragani R. and A.P. McNally, 2013: Operational assimilation of ozone-sensitive infrared radiances at ECMWF. *Q. J. R. Meteorol. Soc.* doi: 10.1002/qj.2106.

Han W. and A.P. McNally 2010: The 4d-var assimilation of ozone-sensitive infrared radiances measured by IASI. *Q. J. R. Meteorol. Soc.* **136**, 2025-2037.

Hólm, E., A. Untch, A. Simmons, R. Saunders, F. Bouttier, E. Andersson, 1999: Multivariate ozone assimilation in 4D data assimilation. SODA Workshop on Chemical Data Assimilation Proceedings.

Hocking, J., R. Saunders, P. Rayer, D. Rundle, P. brunel, J. Vidot, M. Matricardi, A. Geer, and N. Bormann (2012), RTTOV development status, in Proceedings of the 18th international TOVS study conference, Toulouse, France.

Lupu, C. and A.P. McNally, 2012: Assimilation of cloud-affected radiances from Meteosat-9 at ECMWF. EUMETSAT/ECMWF Fellowship Programme Research Reports No.25, 33 pp.

McNally, A., 2009: The direct assimilation of cloud-affected satellite infrared radiances in the ECMWF 4D-Var. *Q. J. R. Meteorol. Soc.*, **135**, 1214-1229.

Peubey C. and A.P. McNally, 2009: Characterization of the impact of geostationary clear-sky radiances on wind analyses in a 4D-Var context. *Q.J.R. Meteorol. Soc.*, **135**, 1863-1876.

Peuch A, J.-N. Thṕaut and J. Pailleux, 2000: Dynamical impact of total-ozone observations in a four-dimensional variational assimilation. *Q. J. R. Meteorol. Soc.* **126**, 1641-1659.

Semane, N., V.-H. Peuch, S. Pradier, G. Desroziers, L. El Amraoui, P. Brousseau, S., Massart, B. Chapnik and A. Peuch, 2009. On the extraction of wind information from the assimilation of ozone proles in Météo-France 4-D-Var operational NWP suite, *Atmos. Chem. Phys.*, **9**, 4855-4867.

Schmetz J., Y. Govaerts, M. Kónig, H.-J Lutz, A. Ratier, S. Tjemkes, 2002. A short introduction to Meteosat Second Generation (MSG), EUMETSAT, 9 pp.

APPENDIX: Accronyms and abbreviations

4D-Var	Four-dimensional variational data assimilation
AIRS	Atmospheric InfraRed Sounder
BUV	Backscatter Ultraviolet
CSR	Clear Sky Radiances
ASR	All Sky Radiances
ECMWF	European Centre for Medium Range Weather Forecast
EUMETSAT	European Organisation for the Exploitation of Meteorological Satellites
FG	First-guess
HIRS	High Resolution Infrared Radiation Sounder
IASI	Infrared Atmospheric Sounding Interferometer
IFS	Integrated Forecasting System
IR	Infrared
MLS	Microwave Limb Sounder
MW	Microwaves
NWP	Numerical Weather Prediction
SBUV/2	Solar Backscatter Ultraviolet Radiometer
SEVIRI	Spinning Enhanced Visible and Infrared Imager
WV	Water vapour